STUDY OF A TURBULENT BOUNDARY LAYER IN A SHORT CHANNEL UNDER THE COMBINED INFLUENCE OF INJECTION THROUGH A POROUS WALL AND ACCELERATION AND TURBULENCE OF THE MAIN FLOW

V. T. Kiril'tsev, V. P. Motulevich, and É. D. Sergievskii

UDC 532.526

Results are presented from measurements of characteristics of a turbulent boundary layer on a porous wall of short, plane channels and an examination is made of features of the calculation of such flows with the use of a "mixing length" model.

As is known [1], channels of various geometries are among the main structural elements of modern power plants which use gas or gas–liquid heat carriers. An effective method of intensifying heat transfer in such units is the use of short channels (of a length $L/D < 30$), in which the local heat-transfer coefficient changes by a factor of two or more. The efficacy of using short channels stems from the fact that it is possible to effectively influence heat transfer through changes in the inlet conditions (such as by changing the level of turbulence) only on the initial sections of the region in which the boundary layer develops. It is in this region that the thermal, concentration, and hydrodynamic boundary layers develop simultaneously. Thus, the study of turbulent boundary layers in short channels with different initial and boundary conditions is a problem of great practical significance. However, the investigator is confronted with serious mathematical complications in any attempt to solve the problem analytically. These complications are aggravated by the fact that the structure of the boundary layer is significantly affected by conditions at the inlet of the channel. There are also methodological difficulties in experimental studies of the problem. These difficulties are due to the fact that it is necessary to perform measurements in thin boundary layers.

The theoretical methods available to date for turbulent boundary layers are semiempirical in nature. Thus, the development and verification of any theoretical analysis require sufficiently accurate and well-documented measurements — mainly measurements of the mean and fluctuation velocity fields.

Our studies were conducted in a wind tunnel with a rectangular working section [2]. The velocity of the main flow at the inlet of the working section was about 20 m/sec in all of the tests. The geometry of the channels was as follows (see Fig. 1): a convergent channel ($dP/dx << 0$) (1), a channel with parallel walls ($dP/dx < 0$) (2), and a channel with a flow regime which approximated as closely as possible a flow with $dP/dx = 0$ (3), i.e., a channel with some divergence. Thus, henceforth channel 3 will be referred to as the divergent channel ($dP/dx \geq 0$). The divergence of channel 3 obviously depends on the injection parameter. Ten holes to sample static pressure (sections 0–IX) were located in one of the side walls of the working section 35 mm from the surface of the porous plate 4. The holes were similar to the holes in [3], which made it possible to minimize the error of static pressure measurement due to flow separation turbulence, and curvature of the flow at these holes and to avoid having to introduce corrections for these measurements. The experimental conditions and the measurement method were similar to those in [4-6].

The main measurements of the characteristics of the turbulent boundary layer were made in sections III, V, and VII with turbulence intensities of 0.35 and 2.25% for the main flow at the channel inlet (we obtained a total of 90 profiles of the longitudinal velocity components). Since bending of the top wall began between sections III and IV, in some cases the flow regime with $dP/dx = 0$ was not reached in section III. This section was chosen for meas-

Moscow Energy Institute. Translated from Inzhenerno-Fizicheskii Zhurnal, Vol. 50, No. 3, pp. 396-405, March, 1986. Original article submitted July 30, 1984.

0022-0841/86/5003-0285$12.50

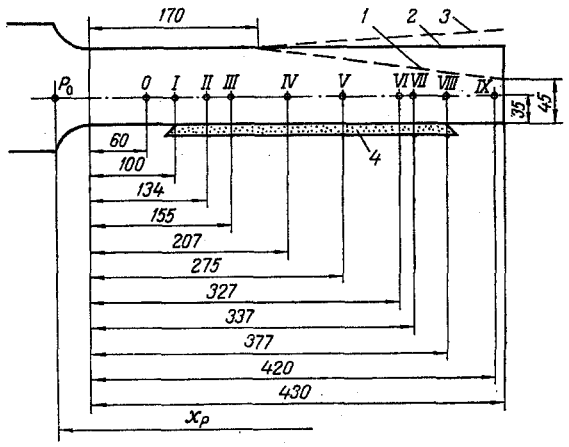

Fig. 1. Geometry of the channels studied.

urement because of the need to evaluate the effect of channel geometry on characteristics of the turbulent boundary layer at the inlet, other conditions being equal.

Figures 2 and 3 show typical measurements obtained in section VII.

Analysis of the empirical data shows that under all of the conditions investigated, an increase in turbulence intensity in the main flow ε_e leads to an increase in the thickness of the boundary layer δ and a decrease in the value of the form parameter $H = \delta_*/\delta_{**}$. These findings are consistent with the results in [17, 18]. The change in the displacement thickness δ_* and momentum thickness δ_{**} here depends on a combination of acceleration and injection parameters. At $K \approx 0$ and $F = 0$ and with flow in the convergent channel ($K = (1.20\text{-}1.65)\cdot 10^{-6}$) at $\bar{F} = 0\text{-}0.01$, an increase in ε_e mainly affects the external part of the profile of mean velocity $\bar{U}$: it becomes "diffuse." (For $K = 0$ and $F = 0$, this is expressed in the familiar reduction in the size of the "wake" region — see Fig. 3c.) The values of δ_* and δ_{**} increase (a similar result was obtained in [7] at $K = 0$ and $F = 0$), but δ_{**} increases more rapidly than δ_* because the form parameter H decreases. At $K = 0$ and $F > 0$, an increase in ε_e is accompanied by noticeable deformation of the entire profile of $\bar{U}$: it becomes fuller (meanwhile, the greater the value of F, the greater the effect of ε_e). This leads to a decrease in δ_* and δ_{**}, despite the fact that the thickness of the boundary layer increases. However, δ_* decreases more rapidly than δ_{**}, since the value of H decreases in this case. A similar result was obtained in [7].

Figure 4 shows certain characteristic results of measurement of mean velocity $\bar{U}$ in section III of the working part of the unit. We should point out the pronounced effect — especially at $F > 0$ — of the channel geometry downflow of section III on the characteristics of the turbulent boundary layer in this section (other conditions being equal). Meanwhile, the change in the profile of mean velocity with the transition from the divergent channel to the convergent channel is similar to the change with an increase in acceleration of the main flow. In fact, this transition is accompanied by a nearly twofold increase in the acceleration parameter K in section III, i.e., a change in the conditions of motion downflow (with constant conditions of motion upflow) restructures the flow field upstream. This is confirmation that the characteristics of the turbulent boundary layer depend on the entire flow field rather than just on local conditions and its history of motion.

The experimental data obtained is of limited value if it is not generalized in the form of some kind of relations which can be used in practical calculations. As was shown in [8-10], the characteristics of a turbulent boundary layer developed on a porous surface with injection and acceleration of the main flow can be calculated with sufficient accuracy by means of a relatively simple model based on the concept of "mixing length." In the opinion of the authors of [8-10], the central part of this model is the expression for A_+ in the Van Dreist decay factor $[1 - \exp(-y_+/A_+)]$. The available relations for A_+ are based on measurements of profiles of the mean velocity $\bar{U}$. The authors of [9] used one of these expressions to reliably describe even such an important fact as the empirically observed but unexpected increase in the Stanton number St with intensive injection and slight acceleration of the main flow (relative to nongradient flow with the same injection and a fixed Reynolds number calculated from the enthalpy thickness), even though each of these factors individually lowers heat transfer.

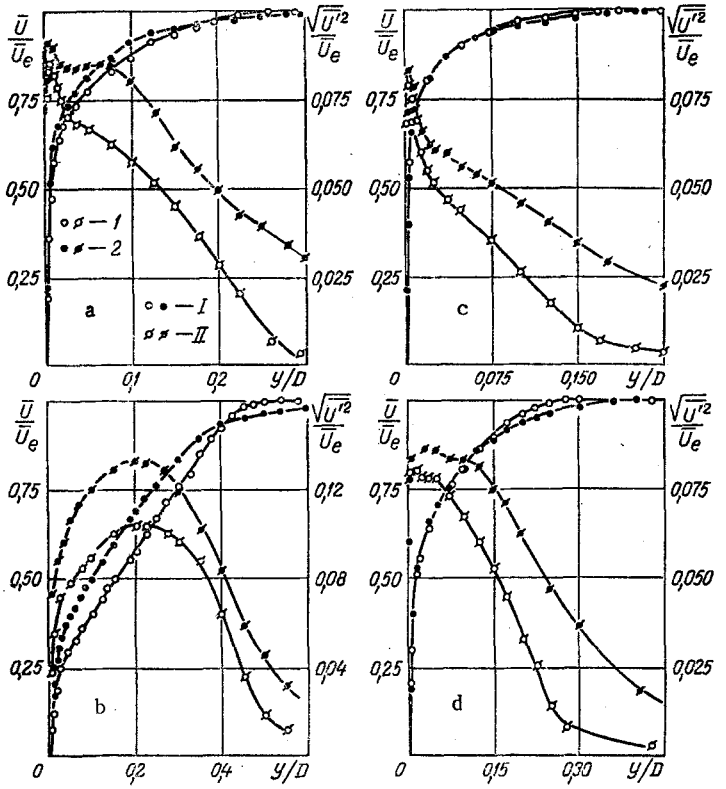

Fig. 2. Profiles of the $\bar{U}$ and $\sqrt{U'^2}$ components of velocity in section VII of the divergent (a, b) and convergent (c, d) channels (I – $\bar{U}/\bar{U}_e$, II – $\sqrt{U'^2}/\bar{U}_e$): a) K = 0, F = 0; 1) ε_e = 0.5%, H = 1.37, Re** = 1284, $C_f = 3.6 \cdot 10^{-3}$; 2) ε_e = 2.5%, H = 1.34, Re** = 1332, $C_f = 3.95 \cdot 10^{-3}$; b) K = 0, F = 0.01; 1) ε_e = 0.5%, H = 2.11, Re** = 4412, $C_f = 0.511 \cdot 10^{-3}$; 2) ε_e = 2.5%, H = 1.85, Re** = 4137, $C_f = 0.751 \cdot 10^{-3}$; c) $K = 1.2 \cdot 10^{-6}$, F = 0; 1) ε_e = 0.35%, H = 1.31, Re** = 800, $C_f = 4.08 \cdot 10^{-3}$; 2) ε_e = 1.6%, H = 1.29, Re** = 846, $C_f = 4.02 \cdot 10^{-3}$; d) $K = 1.38 \cdot 10^{-6}$, F = 0.0076; 1) ε_e = 0.35%, H = 1.5, Re** = 2215, $C_f = 2.03 \cdot 10^{-3}$; 2) ε_e = 1.3%, H = 1.44, Re** = 2455, $C_f = 1.92 \cdot 10^{-3}$. D = 40 mm – width of the channels.

Thus, in [8-10] the effect of injection through a porous surface and acceleration of the main flow on the development of the turbulent boundary layer was generalized in the form of an empirical relation for the Van-Dreist "constant" A_+. As regards the additional effect of turbulence of the main flow, there are still no relations which generalize such a combined effect.

Comparison of the results of numerical calculations using the expression for A_+ proposed in [8] and characteristics of turbulent boundary layers measured under the flow conditions investigated showed that besides the corresponding corrections for the Van Dreist constant, it is necessary to establish the value of the Karman "constant" $\varkappa$ in relation to the boundary conditions. Such a relation is lacking in the literature:

1) The value of $\varkappa$ increases with an increase in the injection parameter F [11] – $\kappa = 11.5\,F + 0.433$ at dP/dx = 0;

2) at dP/dx > 0 (K < 0) and F = 0 the value of $\varkappa$ increases [12-15], while at dP/dx < 0 (K > 0) it decreases [16] relative to $\kappa = 0.4$;

3) at F = 0, an increase in the turbulence intensity of the main flow ε_e is accompanied by an increase in κ [17].

The system of equations, solved numerically by an implicit scheme, has the form

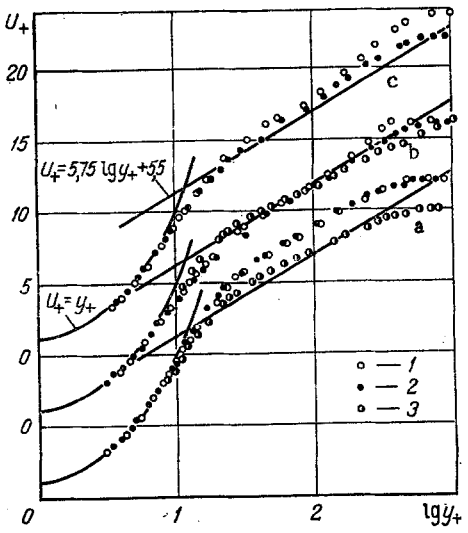

Fig. 3

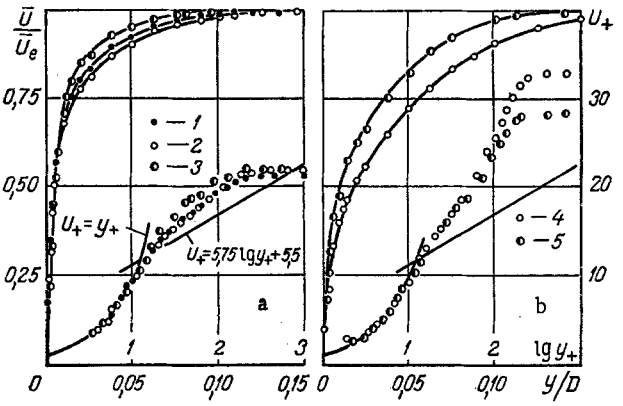

Fig. 4

Fig. 3. Profiles of mean velocity in section VII in the absence of injection: a) 1, 2 — convergent channel ($K = 1.2\cdot10^{-6}$): $\varepsilon_e = 0.35\%$, $Re^{**} = 800$ and $\varepsilon_e = 1.6\%$, $Re^{**} = 846$, respectively; 3) data from [10]: $K = 1.45\cdot10^{-6}$, $\varepsilon_e = 1\%$, $Re^{**} = 775$; b) 1, 2 — channel with parallel walls ($K = 0.21\cdot10^{-6}$): $\varepsilon_e = 0.35\%$, $Re^{**} = 1184$ and $\varepsilon_e = 1.85\%$, $Re^{**} = 1283$, respectively; 3) data from [10]: $K = 0.586\cdot10^{-6}$, $\varepsilon_e = 1\%$, $Re^{**} = 1674$; c) 1, 2 — divergent channel ($K = 0$): $\varepsilon_e = 0.5\%$, $Re^{**} = 1284$ and $\varepsilon_e = 2.5\%$, $Re^{**} = 1332$, respectively.

Fig. 4. Effect of channel geometry on the profile of mean velocity in section III: a) $F = 0$, $\varepsilon_e = 0.35\%$; 1) $K = 0.24\cdot10^{-6}$, $C_f = 4.13\cdot10^{-3}$, $Re^{**} = 517$; 2) $K = 0$, $C_f = 4.2\cdot10^{-3}$, $Re^{**} = 488$; 3) $K = 1.2\cdot10^{-6}$, $C_f = 4.15\cdot10^{-3}$, $Re^{**} = 355$; b) $F \approx 0.01$, $\varepsilon_e = 2.25\%$; 4) $K = 0$, $C_f = 1.83\cdot10^{-3}$, $Re^{**} = 1139$; 5) $K = 1.2\cdot10^{-6}$, $C_f = 2.68\cdot10^{-3}$, $Re^{**} = 743$.

$$\rho\bar{U}\frac{\partial\bar{U}}{\partial x}+\rho\bar{V}\frac{\partial\bar{U}}{\partial y}=-\frac{dP}{dx}+\frac{\partial}{\partial y}\left[(\mu_T+\mu)\frac{\partial\bar{U}}{\partial y}\right],\ \frac{\partial\bar{U}}{\partial x}+\frac{\partial\bar{V}}{\partial y}=0,$$

where

$$\mu_T=\rho l\frac{\partial\bar{U}}{\partial y};\ l=\varkappa\left[1-\exp\left(-\frac{4y}{\delta}\right)\right]\left[1-\exp\left(\frac{y_+}{A_+}\right)\right]\frac{\delta}{4};$$

$$A_+=\frac{26}{N};\ N=\left\{\frac{P_e^+}{V_w^+}[1-\exp(11{,}8V_w^+)]+\exp(11{,}8V_w^+)\right\}^{0,5};$$

$$\varkappa=\varkappa_1\{1+\varkappa_1^2[1-\exp(-k_\varepsilon\varepsilon_e^2)]\}\left\{1+\left[\left(\frac{6000}{Re_{**}}\right)^{0,125}-1\right]\left[1-\exp\left(-\frac{y_+}{A_+}\right)\right]\right\};$$

$$\varkappa_1=\frac{0{,}4+k_FF}{1+k_KK_e};\ P_e^+=-\frac{\nu_e}{\rho U_*^3}\frac{dP_e}{dx};$$

$$K_e=-\frac{\nu_e}{\rho\bar{U}_e^3}\frac{dP_e}{dx};\ V_w^+=\frac{V_w}{U_*}.$$

The empirical coefficients in the proposed corrections for $\varkappa$, accounting for the effect of injection (k_F), acceleration (k_K), and turbulence intensity of the main flow (k_ε), have the following values determined in numerical experiments: $k_F = 15$, $k_\varepsilon = 5\cdot10^2$, $k_K = 2.5\cdot10^4$.

The below follows from the proposed expression for κ.

1. The main effect of ε_e will be manifest in the range up to about 7%, i.e., the changes in ε_e in the calculation will be noticeable in this range and the surface fraction coefficient C_f will undergo its greatest change. These findings are consistent with the conclusions in the experimental studies [18, 19] at $dP/dx = 0$ and $F = 0$. However, as was shown by the experimental studies [20], ε_e is also seen to have an appreciable effect on characteristics of the

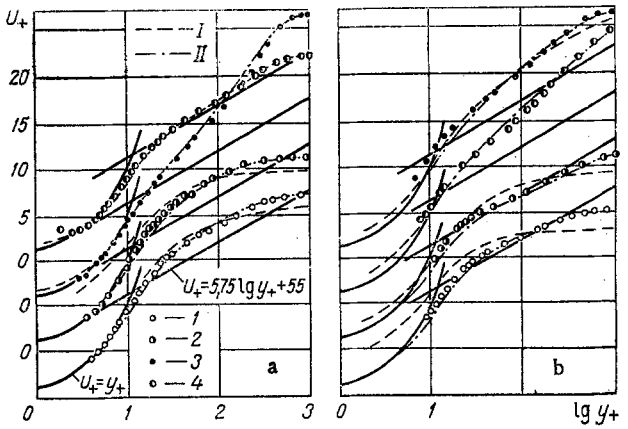

Fig. 5

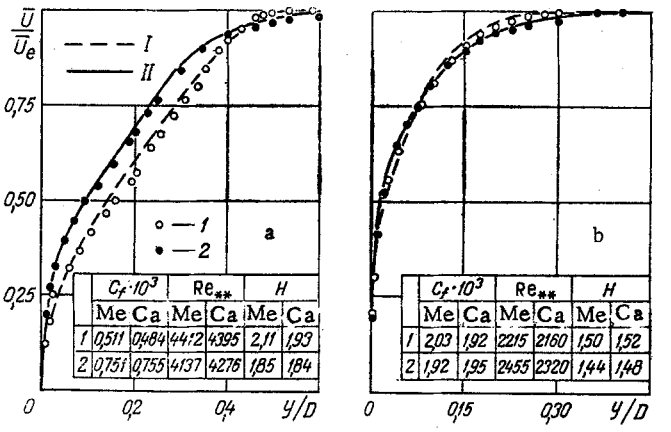

Fig. 6

Fig. 5. Profiles of mean velocity: a) data for the section VII: 1) $K = 1.2 \cdot 10^{-6}$, $F = 0$, $\varepsilon_e = 0.35\%$, $H = 1.31$, $Re^{**} = 800$, $C_f = 4.08 \cdot 10^{-3}$; 2) $K = 1.85 \cdot 10^{-6}$, $F = 0$, $\varepsilon_e = 1.3\%$, $H = 1.35$, $Re^{**} = 525$, $C_f = 4.39 \cdot 10^{-3}$; 3) $K = 1.38 \cdot 10^{-6}$, $F = 0.0076$, $\varepsilon_e = 0.35\%$, $H = 1.5$, $Re^{**} = 2215$, $C_f = 2.03 \cdot 10^{-3}$; 4) $K = 0$, $F = 0$, $\varepsilon_e = 2.5\%$, $H = 1.34$, $Re^{**} = 1332$, $C_f = 3.95 \cdot 10^{-3}$; b) data from [10]: 1) $K = 1.45 \cdot 10^{-6}$, $F = 0$, $\varepsilon_e = 1\%$, $H = 1.24$, $Re^{**} = 775$, $C_f = 496 \cdot 10^{-3}$; 2) $K = 0.586 \cdot 10^{-6}$, $F = 0$, $\varepsilon_e = 1\%$, $H = 1.21$, $Re^{**} = 1674$, $C_f = 438.10^{-3}$; 3) $K = 0.586 \cdot 10^{-6}$, $F = 0.00403$, $\varepsilon_e = 1\%$, $H = 1.32$, $Re^{**} = 3720$, $C_f = 2.14 \cdot 10^{-3}$; 4) $K = 1.44 \cdot 10^{-6}$, $F = 0.00406$, $\varepsilon_e = 1\%$, $H = 1.32$, $Re^{**} = 1688$, $C_f = 2.90 \cdot 10^{-3}$. I) calculation performed from Wheatfield's empirical expression [22]; II) calculation performed from the proposed modification of this expression.

Fig. 6. Calculated and experimental data in section VII: a) divergent channel, $K = 0$, $F = 0.01$: 1) $\varepsilon_e = 0.5\%$, 2) 2.5; b) convergent channel, $K = 1.38 \cdot 10^{-6}$, $F = 0.0076$; 1) $\varepsilon_e = 0.35\%$, 2) 1.3. I) calculated profiles for 1; II) for 2.

turbulent boundary layer at $F > 0$ when $\varepsilon_e > 7\%$. This means that given the proposed expression for κ, the coefficient k_F should depend on ε_e and increase with ε_e. A value $k_F = 15$ was chosen as a first approximation in view of the relatively small range of ε_e in the present experiments.

2. The value of κ in the external region of the turbulent boundary layer depends on the Reynolds number Re^{**} and increases as it decreases (at $Re^{**} > 6000$, we take $Re^{**} = 6000$, i.e., there is no correction for the effect of Re^{**} at $Re^{**} > 6000$). This relation is similar to the well-known dependence of mixing length on Re^{**} [16].

An actual turbulent boundary layer does not react instantly to a change in the longitudinal pressure gradient. There is some lag. This phenomenon was analyzed in [21]. Following [9], we accounted for the phenomenon through an "effective pressure gradient:" in the acceleration parameter K_e and the dimensionless pressure gradient P^+_e used in the expressions for N and κ, we replaced the local pressure gradient dP/dx by a certain "effective" gradient found from the empirical expression

$$\frac{dP_e}{dx} = \frac{dP}{dx} + k_P \frac{P - P_0}{x_P},$$

where P_0 is the static pressure at the initial moment of acceleration of the flow (in the present case, this is the pressure in the inlet main of the wind tunnel directly ahead of the inlet convergent duct); x_P is the distance from the point corresponding to the value of P_0; P is the running value of static pressure. As regards the coefficient k_P, we should expect it to depend on the velocity of the main flow $\bar{U}_e$: the value of k_P should increase with an increase in $\bar{U}_e$, which is equivalent to the effect of the history of the flow over large distances downstream. As the first approximation for $\bar{U}_e \approx 20$ m/sec we took $k_P = 0.3$. The development of the turbulent boundary layer was calculated from section III to section VII of the channels investigated. The initial profile of mean velocity in section III was prescribed by means of the empirical expression

$$U_+ = \frac{1}{0.09}\left\{\operatorname{arctg}(0.09y_+) + \left[\frac{\pi}{2} - \operatorname{arctg}(0.09y_+)\right](y/\delta_0)^4\right\} + \left(U_e^+ - \frac{\pi}{0.18}\right)\sqrt{\operatorname{th}\left[a\,(y/\delta_{**})^{b_1}\right]},$$

where

$$a = \operatorname{arcth}(g_2^2)/2^b;\ b = \ln\left[\frac{\operatorname{arcth}(g_2^2)}{\operatorname{arcth}(g_5^2)}\right]\Big/\ln 0{,}4;\quad b_1 = b\left[1 + 0.475\left(\frac{y}{\delta_0}\right)^4\right],$$

here, if $y > \delta_0$, then we take $y = \delta_0$;

$$g_2 = \frac{U_2 - \frac{1}{0.09U_e^+}\operatorname{arctg}\left(\frac{0.18\,\mathrm{Re}_{**}}{U_e^+}\right)}{1 - \frac{\pi}{0{,}18U_e^+}};$$

$$g_5 = \frac{U_5 - \frac{1}{0.09U_e^+}\operatorname{arctg}\left(\frac{0{,}45\,\mathrm{Re}_{**}}{U_e^+}\right)}{1 - \frac{\pi}{0.18U_e^+}};$$

$$U_2 = 1.72\left(1 + \frac{\Delta R}{\mathrm{Re}_{**}}\right)\exp\left[-0.555H\sqrt{\left(1 + \frac{\Delta R}{\mathrm{Re}_{**}}\right)\left(1 + \frac{1}{G}\right)}\right];$$

$$U_5 = 0.87 + 0.07\left(\frac{G-1}{G+1}\sqrt{\frac{\mathrm{Re}_{**}}{\mathrm{Re}_{**} + \Delta R}}\right)^H;$$

$\delta_0 = \frac{14\delta_{**}}{H}\frac{G+1}{G-1}$ is the "effective" thickness of the turbulent boundary layer; $G = \frac{H-1}{H}U_e^+$ is the Clauser form parameter; $U_e^+ = \bar{U}_e/U_*$; $\Delta R = \left(\frac{1{,}4}{H}\right)^2\left(\frac{H\lg \mathrm{Re}_{**}}{1 + 0.0029\bar{U}_e}\right)^3$.

The parameters U_2 and U_5 represent the quantity $\bar{U}/\bar{U}_e$ at $y/\delta_{**} = 2$ and 5, respectively. The expression for U_+ is a modification of Wheatfield's empirical expression [22]. The expression in [22] differs from the expression here in the additive term $\left[\frac{\pi}{2} - \operatorname{arctg}(0{,}09y_+)\right](y/\delta_0)^4$, the exponent with y/δ_{**}, and the expressions for the velocities U_2 and U_5.

Figure 5 compares experimental data with results calculated from the initial expression of Wheatfield [22] and its proposed modification. The presence of acceleration in the main flow obviously improves the agreement between the experimental profile and the profile calculated from the modification of Wheatfield's empirical expression (one curve was drawn where both calculated profiles are close to each other). The friction velocity U* was determined by the method in [4].

Figure 6 compares results of the numerical calculation and the experiment in section VII of the divergent and convergent channels. It can be seen that the agreement is satisfactory.

Thus, the combined effect of injection through a porous surface and acceleration and turbulence in the main flow on the development of a turbulent boundary layer can be generalized in the form of dependences of the Van Dreist and Karman "constants" on the boundary conditions of the flow.

NOTATION

$\bar{U}$ and $\sqrt{\overline{U'^2}}$, mean and fluctuation components of longitudinal velocity; $\bar{V}$, mean transverse velocity; $\varepsilon = \sqrt{\overline{U'^2}}/\bar{U}$, turbulence intensity; $K = -\frac{\nu_e}{\bar{\rho}_e\bar{U}_e^3}\frac{dP}{dx}$, acceleration parameter; $F = \frac{\rho_w V_w}{\bar{\rho}_e\bar{U}_e}$, injection parameter; $P^+ = -\frac{\nu_e}{\rho_e U_*^3}\frac{dP}{dx}$, dimensionless pressure gradient; ρ, density, U*, friction velocity; $\mathrm{Re}_{**} = \delta_{**}\bar{U}_e/\nu_e$; δ, δ_* and δ_{**}, thickness of the boundary layer, displacement thickness, and momentum thickness, respectively; C_f, local surface friction coefficient; μ, dynamic viscosity; $\nu = \mu/\rho$, kinematic viscosity; $U_+ = \bar{U}/U_*$; $y_+ = yU_*/\nu$; l, mixing length; κ and A_+, Karman and Van Dreist "constant;" P, static pressure. Indices: t, turbulent; w, wall; e, main flow (or pertaining to "effective pressure gradient").

LITERATURE CITED

1. A. S. Sukomel, V. I. Velichko, and Yu. G. Abrosimov, Heat Transfer and Friction in the Turbulent Flow of Gas in Short Channels [in Russian], Énergiya, Moscow (1979).
2. V. T. Kiril'tsev, V. P. Motulevich, and E. D. Sergivskii, "Wind tunnel for experimental study of the characteristics of a boundary layer," Tr. Mosk. Energ. Inst., No. 491, "Problems of Thermodynamics and Heat Transfer in Low-Temperature Units" (1980), pp. 85-97.
3. Hussein and Reynolds, "Experimental study of a fully developed turbulent flow in a channel," Teor. Osn. Inzh. Raschetov, No. 4, 295-309 (1975).
4. V. T. Kiril'tsev, V. P. Motulevich, and E. D. Sergievskii, "Some data on the structure of the wall region of a turbulent boundary layer on a permeable surface with injection," Inzh.-Fiz. Zh., 50, No. 1, 22-29 (1986).
5. V. T. Kiril'tsev, V. P. Motulevich, and E. D. Sergievskii, "Effect of mean flow temperature on the readings of a hot-wire anemometer," Inzh.-Fiz. Zh., 42, No. 4, 622-627 (1982).
6. V. T. Kiril'tsev, V. P. Motulevich, and E. D. Sergievskii, "Hot-wire anemometer measurements in highly turbulent boundary layers," Promyshlennaya Teplotekhnika, 4, No. 5, 96-101 (1982).
7. A. I. Alimpiev and V. I. Alimpiev, "Turbulent boundary layer on a rough permeable surface," in: Turbulent Boundary Layer with Complex Boundary Conditions [in Russian], Inst. Teplofiz. Sib. Otd. Akad. Nauk SSSR, Novosibirsk (1977), pp. 49-59.
8. Sebesi, "Turbulent flow near a porous wall in the presence of a pressure gradient," Raket. Tekh. Kosmon., No. 12, 48-53 (1970).
9. Case, Moffat, and Tilbar, "Heat transfer in the turbulent boundary layer of a highly accelerated flow with injection and suction," Teploperedacha, No. 3, 190-198 (1970).
10. Julien, Case, and Moffat, "Experimental study of a turbulent boundary layer with suction and injection in a flow with acceleration," Teploperedacha, No. 4, 51-59 (1971).
11. Isaakson and Christiansen, "Equation of turbulence kinetic energy for a turbulent boundary layer in the presence of injection," Raket. Tekh. Kosmon., No. 3, 229-231 (1971).
12. Sturek, "Shear stress distribution in a turbulent boundary layer for a compressible flow with a positive pressure gradient," Raket. Tekh. Kosmon., No. 3, 149-150 (1974).
13. C. E. Jobe and W. L. Hankey, "Turbulent boundary layer calculation in adverse pressure gradient flow," AIAA Paper, No. 136, 1-8 (1980).
14. P. Bradshaw, "The turbulence structure of equilibrium boundary layers," J. Fluid Mech., 29, Pt. 4, 625-645 (1967).
15. S. Patankar and D. Spalding, Heat and Mass Transfer in Boundary Layers [Russian translation], Énergiya, Moscow (1971).
16. P. Bradshaw (ed.), Turbulence [Russian translation], Mashinostroenie, Moscow (1980).
17. A. N. Sherstyuk and T. V. Shul'gina, "Calculation of the characteristics of a boundary layer with allowance for the effect of turbulence in the external flow," Teploenergetika, No. 9, 43-45 (1979).
18. B. P. Mironov, A. I. Alimpiev, A. A. Zelengur, et al., "Experimental characteristics of a turbulent boundary layer on a permeable surface," in: Turbulent Boundary Flow: Transactions of the XVIII Siberian Thermophysical Seminar. Part 2. Inst. Teplofiz. Sib. Otd. Akad. Nauk SSSR, Novosibirsk (1975), pp. 7-29.
19. E. P. Dyban and E. Ya. Epik, "Microstructure of boundary layers and transport processes in them with increased turbulence in the external flow," in: Turbulent Boundary Flow: Transactions of the SVII Siberian Thermophysical Seminar. Part 2. Inst. Teplofiz. Sib. Otd. Akad. Nauk SSSR, Novosibirsk (1975), pp. 30-42.
20. A. I. Alimpiev, V. N. Mamonov, and A. L. Sorokin, "Turbulent boundary layer on a permeable plate with different degrees of turbulence in the incoming flow," in: Some Problems of Hydrodynamics and Heat Transfer, Inst. Teplofiz. Sib. Otd, Akad. Nauk SSSR, Novosibirsk (176), pp. 143-148.
21. Horstmen, "Model of turbulence for calculating nonequilibrium flows with a positive pressure gradient," Raket. Tekh. Kosmon. No. 2, 5-7 (1977).
22. Wheatfield, "Analytical description of the complete velocity profile in a turbulent boundary layer," Raket. Tekh. Kosmon., No. 10, 154-156 (1979).